Biophysical Chemistry 193–194 (2014) 9–19

Contents lists available at ScienceDirect

Biophysical Chemistry

journal homepage: http://www.elsevier.com/locate/biophyschem

Competitive inhibition reaction mechanisms for the two-step model of protein aggregation

Mark Whidden [a], Allison Ho [a], Magdalena I. Ivanova [b], Santiago Schnell [a,c,d,*]

[a] Department of Molecular & Integrative Physiology, University of Michigan Medical School, Ann Arbor, MI 48109, USA
[b] Department of Neurology, University of Michigan Medical School, Ann Arbor, MI 48109, USA
[c] Department of Computational Medicine and Bioinformatics, University of Michigan Medical School, Ann Arbor, MI 48109, USA
[d] Brehm Center for Diabetes Research, University of Michigan Medical School, Ann Arbor, MI 48105, USA

HIGHLIGHTS

- Three mechanisms for competitive inhibition of protein aggregation are introduced.
- Rate equations are derived to estimate aggregation inhibition constants.
- Rate equations are used to distinguish inhibition mechanisms of insulin aggregation.
- Longer insulin peptide inhibitors delay insulin aggregation onset.
- Shorter insulin peptide inhibitors reduce total concentration of aggregated insulin.

GRAPHICAL ABSTRACT

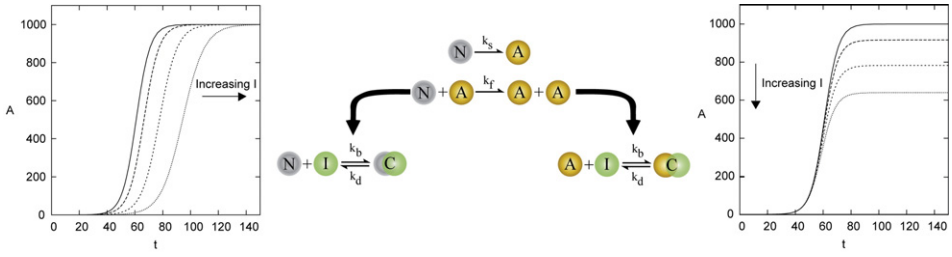

ARTICLE INFO

Article history:
Received 29 March 2014
Received in revised form 22 June 2014
Accepted 27 June 2014
Available online 5 July 2014

Keywords:
Protein aggregation
Reaction mechanism
Inhibition
Kinetic result analysis
Distinguishing inhibition mechanism
Parameter estimation

ABSTRACT

We propose three new reaction mechanisms for competitive inhibition of protein aggregation for the two-step model of protein aggregation. The first mechanism is characterized by the inhibition of native protein, the second is characterized by the inhibition of aggregation-prone protein and the third mechanism is characterized by the mixed inhibition of native and aggregation-prone proteins. Rate equations are derived for these mechanisms, and a method is described for plotting kinetic results to distinguish these three types of inhibitors. The derived rate equations provide a simple way of estimating the inhibition constant of native or aggregation-prone protein inhibitors in protein aggregation. The new approach is used to estimate the inhibition constants of different peptide inhibitors of insulin aggregation.

1. Introduction

Surveillant processes that control protein quality (proteostasis) are critical for functionality and longevity of the cell [1]. Under optimal physiological conditions, protein homeostasis may be viewed as a dynamic network of interconnected processes which are monitored and regulated by quality control mechanisms, ameliorating any instances of inappropriate folding or oligomerization [2]. When the cellular surveillance of protein quality is compromised, proteins start to form misfolded species that are associated with a variety of diseases, many of which are terminal. Therefore, understanding the mechanisms by which proteins aggregate is of paramount importance for the development of effective methods to ameliorate protein folding diseases.

* Corresponding author at: Department of Molecular & Integrative Physiology, University of Michigan Medical School, Ann Arbor, MI 48109, USA.
E-mail address: schnells@umich.edu (S. Schnell).

http://dx.doi.org/10.1016/j.bpc.2014.06.006
0301-4622/

Misfolding and aggregation can also occur in proteins synthesized industrially. Biosynthetic human insulin is manufactured for widespread clinical treatment of diabetes, but its aggregation in vitro and in the bloodstream makes it pharmacologically ineffective [3–5]. Observations of oligomerization, aggregation and amyloid fibrillogenesis from misfolded proteins have prompted explorations into inhibitory compounds that either prevent unfolding of the native protein or sequester partially folded aggregation-prone intermediates [3].

Misfolded or aggregation-prone proteins have been described as intrinsically disordered proteins, lacking a defined, stable, structured state [6]. In vitro studies have found a correlation between protein stability and aggregation propensity [7–9]. In general, partial unfolding and destabilization of the protein due to mutations or environmental changes increase the aggregation propensity of the protein.

Oosawa and Asakura [10] presented one of the first monographs of protein polymerization and aggregation in 1975. Classical studies of protein aggregation combined kinetics and thermodynamics when attempting to understand the mechanism of protein aggregation [11,12]. Eaton and Hofrichter [13] explicitly employ reaction kinetics to investigate the mechanisms of hemoglobin S gelation both in vitro and in vivo. They also accounted for temperature and pressure to infer the mechanisms of hemoglobin S aggregation [14].

In this work, we focus our attention on the reaction kinetics of the time course of aggregation-prone species to infer minimalistic reaction mechanisms of protein aggregation. In 1997, Watzky and Finke [15] proposed a minimalistic two-step model of protein aggregation which was inspired by classical mechanistic literature from the 1950s on the formation of colloids in homogeneous, initially supersaturated solutions by LaMer [16,17]. The model is also known as the Finke–Watzky two-step model (F–W model) or "Ockham's razor"/minimalistic F–W model [18,19]. In the first step, native protein N is converted with a slow first-order rate into aggregation-prone protein A. The second step is a fast second-order autocatalytic, irreversible conversion of N into A by using an existing A as a template. The reaction scheme for the two-step model is:

$$\begin{aligned} N &\xrightarrow{k_s} A \\ N + A &\xrightarrow{k_f} 2A \end{aligned} \tag{1}$$

where k_s and k_f are rate constants. This reaction scheme has been successfully used to describe the time course of protein aggregation for numerous proteins, including amyloid β, α-synuclein, polyglutamine, prions, and human calcitonin aggregation [15,19,20]. It has also been applied to investigate aggregation inhibition [3]. A limitation of using reaction scheme Eq. (1) to characterize aggregation inhibitors is that it does not explicitly account for the presence of inhibitors and hence neglects the mechanism of inhibition, which is essential to the design of highly specific pharmacological agents [21,22].

We introduce three competitive inhibition reaction mechanisms to the F–W model of protein aggregation Eq. (1). These inhibition mechanisms differ in the assumption that a given inhibitor binds with high specificity to native protein, aggregation-prone protein, or both proteins. We derive rate expressions for the time course and initial rates of the aggregation-prone species formation, which allow the estimation of inhibition constants. We also derive conditions for the validity of our rate equations. We test and validate our rate expressions by studying time courses of the inhibition of aggregation using insulin as an example. This demonstrates how the competitive inhibition mechanisms can be used to model experimental data.

2. The Finke–Watzky two-step model of protein aggregation

Watzky and Finke introduced a two-step model described by the reaction scheme Eq. (1) in 1997 [15,19]. They used this model to study the transition-metal nanocluster formation through two pseudoelementary steps [15,18,19,23]. Thereafter, Finke and colleagues fit the F–W model to 41 kinetic data sets from the literature [18,23]. Fourteen of these kinetic data sets were amyloid protein aggregation [23]. The excellent fit of these 14 data sets with R^2 values larger than or equal to 0.98 showed the wide applicability of the F–W model. Next, Watzky et al. [18] fit the F–W model to 27 prion aggregation kinetic data sets. All 27 fits were good to excellent with a range of R^2 values from 0.764 to 0.999 [18]. The application of the F–W model to 41 kinetic data sets demonstrates the power of minimalistic modeling of aggregation systems with a fully quantifiable model [18,23].

The F–W model was also independently proposed by Saitô and colleagues in 2000 for the fibrillation mechanism of calcitonin as a three-step model that is mathematically identical to the F–W model [20,23]. Thereafter, more researchers used Saitô's version of the F–W model to fit β-amyloid aggregation [24–27] and HET-s, a fungal prion protein [28]. In 2006, Gibson and Murphy [3] used the F–W model to describe the time course of insulin aggregation in the presence of inhibitors.

Applying the law of mass action to reaction scheme Eq. (1), the governing differential equations for the F–W model are:

$$\begin{aligned} \frac{dn}{dt} &= -k_s n - k_f n a \\ \frac{da}{dt} &= k_s n + k_f n a. \end{aligned} \tag{2}$$

where n is the concentration of native protein species N and a is the concentration of aggregation-prone species A. Using the law of mass conservation for the reaction scheme,

$$\frac{dn}{dt} + \frac{da}{dt} = 0, \tag{3}$$

the system Eq. (2) can be analytically solved to obtain a closed-form expression for a as a function of time:

$$a(t) = \frac{n_0\left(e^{k_s t(1+kn_0)} - 1\right)}{kn_0 + e^{k_s t(1+kn_0)}}, \tag{4}$$

where n_0 is the initial concentration of native protein, and $k = k_f/k_s$. In the above expression, it is assumed that aggregates are initially absent from the reaction.

3. Competitive inhibitors of protein aggregation

Given the broad range of pathological conditions and industrial problems associated with aggregation of proteins, there is a great interest in exploring strategies that prevent or delay the onset of protein aggregation. This can occur by either intrinsically modifying the amino acid sequence of the protein or by pharmacologically altering the extrinsic reaction environment of proteins [29]. Structural modifications can be performed by site-specific mutagenesis [30] or by chemical reactions [31]. However, these intrinsic modifications can affect the functional activity of the protein – a problem that may, in many cases, be intractable.

On the other hand, there has been considerable attention paid to enhancing the structural integrity of proteins by changing the local milieu of the protein. This is commonly accomplished by the introduction of excipients or additives to stabilize proteins by preferential interactions, so that aggregation is inhibited [32,33]. For instance, molecules that alter insulin aggregation include lecithins, cyclodextrins, and polymeric surfactants [34–37], carbohydrates and glycerols [38–40], low molecular weight compounds such as betaine, trehalose, and citrulline [41], and small hybrid peptides [3].

The kinetic characterization of inhibitors is a valuable tool for investigating the mechanisms of aggregation, and it is also of practical importance in the search, design and characterization of protein aggregation

inhibitors. These inhibitors can exhibit different mechanisms of action, which depend on the structural properties of proteins and inhibitors. In this paper, we systematically analyze three types of competitive inhibition mechanisms for the F–W model of protein aggregation Eq. (1): inhibition of native protein, inhibition of aggregation-prone protein, and inhibition of both native and aggregation-prone proteins. These inhibition mechanisms differ in the assumption that a given inhibitor binds with high specificity to native protein, aggregation-prone protein, or both proteins.

3.1. Reversible competitive inhibition of native protein

In this mechanism, the inhibitor I reversibly binds to a native protein forming a complex C, thereby sequestering native protein and delaying its aggregation. The reaction scheme of this inhibition mechanism is given by

$$\begin{aligned} &N \xrightarrow{k_s} A \\ &N + A \xrightarrow{k_f} 2A \\ &N + I \underset{k_d}{\overset{k_b}{\rightleftharpoons}} C \end{aligned} \tag{5}$$

where k_b and k_d are rate constants for the association and dissociation of the native–inhibitor complex, respectively. Applying the law of mass action, this yields the following system of differential equations:

$$\frac{dn}{dt} = -k_s n - k_f n a - k_b n i + k_d c \tag{6}$$

$$\frac{da}{dt} = k_s n + k_f n a \tag{7}$$

$$\frac{di}{dt} = -k_b n i + k_d c \tag{8}$$

$$\frac{dc}{dt} = k_b n i - k_d c. \tag{9}$$

where i is the concentration of inhibitor species I, and c is the concentration of native–inhibitor complex species C. Here, a and c are initially zero, and n_0 and i_0 are the initial concentrations (in arbitrary units) of native proteins and inhibitors, respectively.

The above model has two conserved quantities, which we exploit to simplify the dimensionality of the differential equation system:

$$\frac{dn}{dt} + \frac{da}{dt} + \frac{dc}{dt} = 0 \tag{10}$$

$$\frac{di}{dt} + \frac{dc}{dt} = 0 \tag{11}$$

which implies that

$$n = n_0 - a - c \tag{12}$$

$$i = i_0 - c. \tag{13}$$

Substituting Eqs. (12) and (13) into Eqs. (7) and (9) yields

$$\frac{da}{dt} = k_s(n_0 - a - c) + k_f(n_0 - a - c)a \tag{14}$$

$$\frac{dc}{dt} = k_b(n_0 - a - c)(i_0 - c) - k_d c. \tag{15}$$

If the rate of native–inhibitor complex formation is fast, and the complex is a short-lived intermediate, we can assume that the native–inhibitor complex reaches a rapid equilibrium after a brief initial transient phase. This allows us to simplify the rate equations governing the reversible competitive inhibition of native protein. Under the rapid equilibrium assumption, we take $dc/dt \approx 0$, for which Eq. (15) can be written as

$$0 = c^2 - (k_i + i_0 + n_0 - a)c + i_0(n_0 - a) \tag{16}$$

where $k_i = k_d/k_b$. The solutions of Eq. (16) are given by

$$c = \frac{1}{2}\left[(k_i + i_0 + n_0 - a) \pm \sqrt{(k_i + i_0 + n_0 - a)^2 - 4i_0(n_0 - a)}\right]. \tag{17}$$

We rewrite Eq. (17) for c as

$$c = \frac{1}{2}(k_i + i_0 + n_0 - a)\left[1 \pm \sqrt{1 - \frac{4i_0(n_0 - a)}{(k_i + i_0 + n_0 - a)^2}}\right]. \tag{18}$$

Quadratic expressions similar to Eq. (18) are common in chemical kinetics. For practical use in the analysis of chemical kinetics experiments, quadratic expressions are generally replaced with simpler expressions. Noting that

$$\epsilon = \frac{4i_0(n_0 - a)}{(k_i + i_0 + n_0 - a)^2} \ll 1 \tag{19}$$

for any value of a (for more details, see Appendix A), we can then obtain a Taylor expansion of Eq. (18) to obtain two solution branches of the quadratic expression as

$$c^+ = \frac{1}{2}(k_i + i_0 + n_0 - a)\left[2 - \frac{1}{2}\epsilon + \mathcal{O}\left(\epsilon^2\right)\right] \tag{20}$$

$$c^- = \frac{1}{2}(k_i + i_0 + n_0 - a)\left[\frac{1}{2}\epsilon + \mathcal{O}\left(\epsilon^2\right)\right]. \tag{21}$$

If the inhibitor is initially absent ($i_0 = 0$), Eq. (20) does not recover the simplified model given by Eq. (2). Therefore, this branch is considered unphysical, and we assume c is given by Eq. (21). Substitution of Eq. (21) into Eq. (14) reveals

$$\frac{da}{dt} = \frac{\left(k_s + k_f a\right)\left(n_0 - a\right)}{1 + \frac{i_0}{k_i + n_0 - a}}. \tag{22}$$

Here, if $i_0 = 0$ in Eq. (22), then the expression can be solved in a closed form identical to Eq. (4). As such, Eq. (22) results from a logical extension of the F–W model given by reaction scheme Eq. (1), which explicitly includes and characterizes the reversible competitive inhibition of the native protein during protein aggregation. The rate Eq. (22) can be used to estimate the kinetics parameters from the nonlinear fitting of progress curves experiments. In these experiments, the concentration of the aggregation-prone species is recorded in time after the initial fast transient and for a sufficiently long period to allow the reaction to be completed.

An alternative experimental approach is to estimate the kinetics parameters from initial rate experiments. In these experiments, rates are measured for a short period after the attainment of the rapid equilibrium of the native–inhibitor reaction, typically by monitoring the accumulation of aggregation-prone species with time. Because the measurements are carried out for a very short period, the

approximation $a \approx 0$ can be made. Applying this approximation to Eq. (22) leads to the initial rate of the aggregation-prone species formation

$$v_0 = \frac{da}{dt} = \frac{k_s n_0}{1 + \frac{i_0}{k_i + n_0}}. \tag{23}$$

If the inhibitor is absent, $i_0 = 0$, then this reduces to

$$v_0 = k_s n_0, \tag{24}$$

which implies that the initial rate is linear with respect to the initial native protein concentration. By measuring the initial rate varying n_0, it is possible to estimate k_s by a linear regression. Clearly, in the presence of inhibitor, the value of v_0 in Eq. (23) strictly decreases as k_i decreases, i.e. the initial rate of aggregation decreases with stronger inhibitory compounds. The estimated value of k_s from linear regression of aggregation without inhibitor, along with varying n_0 and i_0, can be used to obtain estimates for k_i.

3.2. Reversible competitive inhibition of aggregation-prone protein

Now, we recast our analysis for the case of the inhibitor I reversibly associating with an aggregation-prone protein A to form a complex C, thereby preventing aggregation by sequestering aggregation-prone proteins. In this case, the reaction scheme is given by

$$\begin{aligned} N &\xrightarrow{k_s} A \\ N + A &\xrightarrow{k_f} 2A \\ A + I &\underset{k_d}{\overset{k_b}{\rightleftharpoons}} C \end{aligned} \tag{25}$$

where again k_b and k_d are rate constants for the association and dissociation of the aggregation-prone–inhibitor complex, respectively. This yields the following system of differential equations:

$$\frac{dn}{dt} = -k_s n - k_f n a \tag{26}$$

$$\frac{da}{dt} = k_s n + k_f n a - k_b a i + k_d c \tag{27}$$

$$\frac{di}{dt} = -k_b a i + k_d c \tag{28}$$

$$\frac{dc}{dt} = k_b a i - k_d c. \tag{29}$$

This reaction has the same initial conditions and conservation laws as the reversible competitive inhibition of native proteins (Section 3.1). Substituting Eqs. (12) and (13) into Eqs. (27) and (29) yields

$$\frac{da}{dt} = k_s(n_0 - a - c) + k_f(n_0 - a - c)a - k_b a(i_0 - c) + k_d c \tag{30}$$

$$\frac{dc}{dt} = k_b a(i_0 - c) - k_d c. \tag{31}$$

Similarly, assuming that the aggregation-prone–inhibitor complex achieves rapid equilibrium after a fast initial transient phase, we take $dc/dt \approx 0$, for which Eq. (31) can be written as

$$0 = k_b a(i_0 - c) - k_d c. \tag{32}$$

This gives a unique solution for c in terms of a as

$$c = \frac{i_0 a}{k_i + a}. \tag{33}$$

Upon substitution of Eq. (33) into Eq. (30), we obtain a rate equation for the aggregation-prone protein formation

$$\frac{da}{dt} = \left(k_s + k_f a\right)\left(n_0 - a - \frac{i_0 a}{k_i + a}\right). \tag{34}$$

Similar to the analysis in Section 3.1, in the absence of inhibitor (i.e. $i_0 = 0$), Eq. (34) recovers the solution of the F–W model given by Eq. (4).

The above expression can be used to estimate the kinetics parameters in progress curves experiments. For initial rate experiments, we make $a \approx 0$. This leads to the initial rate of aggregation-prone protein formation of the form

$$v_0 = \frac{da}{dt} = k_s n_0. \tag{35}$$

Note that, in the case of inhibition of aggregation-prone protein, the initial rate of aggregation-prone protein formation, under the rapid equilibrium, assumption is independent of the inhibitor concentration.

3.3. Mixed reversible competitive inhibition

Here, we consider the reversible mixed inhibition mechanism, in which an inhibitor can bind to both native protein and aggregation-prone protein. In this case, the reaction scheme is given by

$$\begin{aligned} N &\xrightarrow{k_s} A \\ N + A &\xrightarrow{k_f} 2A \\ N + I &\underset{k_{dN}}{\overset{k_{bN}}{\rightleftharpoons}} C_1 \\ A + I &\underset{k_{dA}}{\overset{k_{bA}}{\rightleftharpoons}} C_2 \end{aligned} \tag{36}$$

where k_{dN} and k_{bN} are the dissociation and binding rates of the native–inhibitor complex and k_{dA} and k_{bA} are the dissociation and binding rates of the aggregation-prone–inhibitor complex. Applying the law of mass action, we derive the governing equations for the mixed inhibition case:

$$\frac{dn}{dt} = -k_s n - k_f n a - k_{bN} n i + k_{dN} c_1 \tag{37}$$

$$\frac{da}{dt} = k_s n + k_f n a - k_{bA} a i + k_{dA} c_2 \tag{38}$$

$$\frac{di}{dt} = -k_{bN} n i + k_{dN} c_1 - k_{bA} a i + k_{dA} c_2 \tag{39}$$

$$\frac{dc_1}{dt} = k_{bN} n i - k_{dN} c_1 \tag{40}$$

$$\frac{dc_2}{dt} = k_{bA} a i - k_{dA} c_2. \tag{41}$$

If n and i are the only chemical species present initially, we denote their initial concentrations n_0 and i_0, respectively.

Following the same analysis carried out for the competitive inhibition of native protein (Section 3.1) and the competitive inhibition of aggregation-prone protein (Section 3.2), it is possible to derive a rate

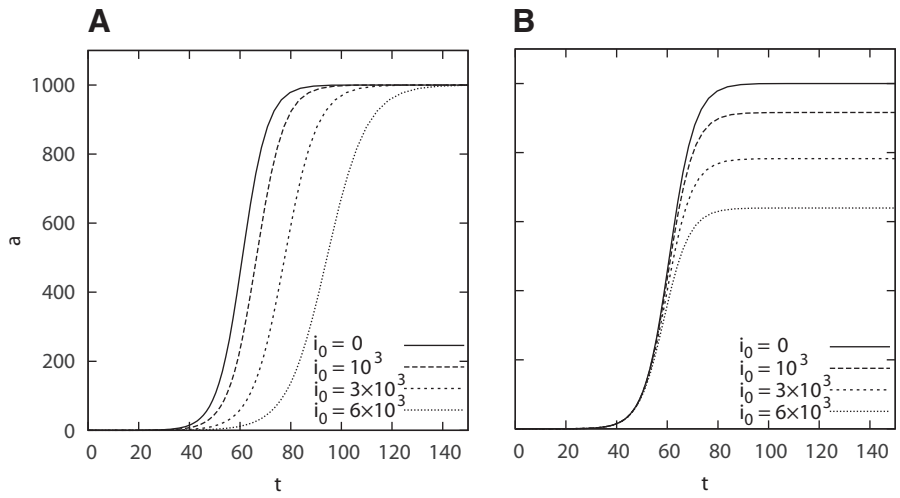

Fig. 1. Time course of the aggregation-prone protein concentration a for the reversible competitive inhibition of native proteins Eq. (5) [Panel A] and reversible competitive inhibition of aggregation-prone proteins Eq. (25) [Panel B]. The inhibitor delays the formation of aggregation-prone proteins in the reversible competitive inhibition of native proteins. In contrast, the presence of the inhibitor decreases the total concentration of aggregation-prone species formed in the reversible competitive inhibition of aggregation-prone proteins. The time course of these reactions is governed by Eqs. (22) and (34), respectively. The parameter values are: $k_s = 1\times10^{-6}$, $k_f = 2\times10^{-4}$, $k_i = 1\times10^4$, $a_0 = 0$, and $n_0 = 1000$. Units are arbitrary and chosen for illustrative purposes.

expression for the aggregation-prone protein formation using the rapid-equilibrium assumption. However, the rate equation is a complicated analytic formula which is not practical for use in the analysis of kinetics experiments. In lieu of this, we limit our analysis of this mechanism to numerical investigations of the aggregation-prone protein formation in the following section.

4. Distinguishing the type of aggregation inhibition

Plotting the progress curves of aggregation-prone proteins for each reversible competitive inhibition mechanism, governed by Eqs. (22), (34) and (38), can be used to distinguish the type of inhibition mechanism in an aggregation reaction. For example, if the time course of a is plotted for several values of i_0, we can observe qualitative differences in the reaction dynamics between the competitive inhibition of native proteins and competitive inhibition of aggregation-prone proteins (Fig. 1). These same comparative features can also be observed if the time course of a is plotted for several values of k_i (Fig. 2).

When the inhibitor specifically binds with native proteins, then a will asymptotically approach a plateau given by n_0. All of the native protein species will eventually convert to aggregation-prone species by direct conversion or autocatalytic interaction with aggregation-prone proteins. However, the effect of inhibition is transient as the inhibitors reversibly sequester native proteins from these two events. This causes a delay in the onset of aggregation.

On the other hand, if the inhibitor specifically binds aggregation-prone species, then a will asymptotically approach a value that is lower than n_0. The equilibrium state of a in Eq. (34) is given by

$$\lim_{t\to\infty} a = \frac{1}{2}\left(n_0 - i_0 - k_i + \sqrt{(n_0 - i_0 - k_i)^2 + 4n_0k_i}\right).$$

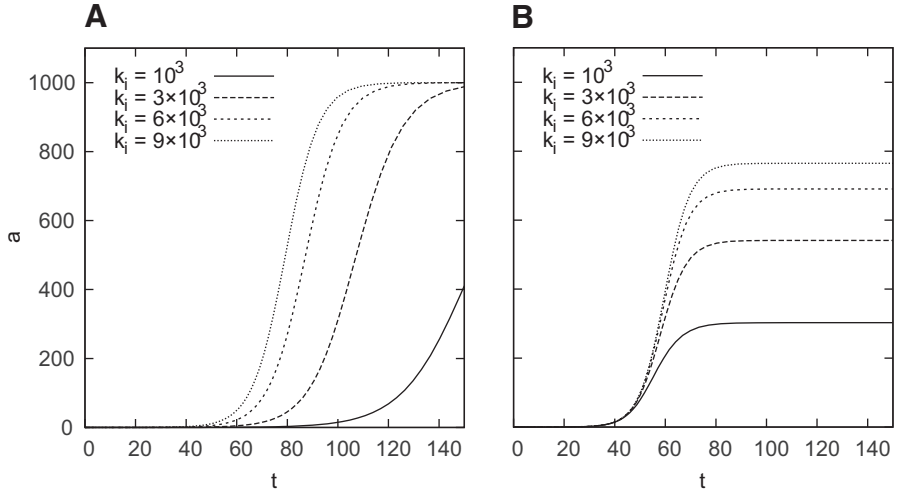

Fig. 2. Time course of the aggregation-prone protein concentration a for the reversible competitive inhibition of native proteins Eq. (5) [Panel A] and reversible competitive inhibition of aggregation-prone proteins Eq. (25) [Panel B]. Stronger inhibitors (lower values of k_i) delay the formation of aggregation-prone proteins in the reversible competitive inhibition of native proteins. In contrast, the stronger inhibitors decrease the total concentration of aggregation-prone species formed in the reversible competitive inhibition of aggregation-prone proteins. The time course of these reactions is governed by Eqs. (22) and (34). The parameter values are: $k_s = 1\times10^{-6}$, $k_f = 2\times10^{-4}$, $i_0 = 3000$, $a_0 = 0$, and $n_0 = 1000$. Units are arbitrary and chosen for illustrative purposes.

This restriction on the accumulation of aggregation-prone proteins at long times can be exploited pharmacologically to maintain sustainable levels of aggregation-prone protein, below a proteotoxic threshold. Furthermore, the specificity of the inhibitor for aggregation-prone proteins may be useful for the design of therapeutic strategies for the degradation of only aggregation-prone proteins. However, the behavior at the initial stages of aggregation is unaffected for the competitive inhibition of aggregation-prone species.

An alternative approach to distinguish between the competitive inhibition of native proteins Eq. (5) and competitive inhibition of aggregation-prone proteins Eq. (25) for the two-step model of protein aggregation is through initial rate experiments. The approach will require estimating the initial velocity of the reaction for different values of n_0 at several values of i_0. As we noted in Section 3.2, the initial rate of aggregation-prone species formation is independent of the inhibitor concentration in the competitive inhibition of aggregation-prone protein. On the other hand, the initial rate of aggregation-prone species formation is dependent on the inhibitor concentration in the competitive inhibition of native protein. From the biochemical point of view, it is reasonable that the initial rate of aggregation-prone species formation is independent of the inhibitor concentration in the competitive inhibition of aggregation-prone protein. In this case, inhibitors specifically associate with aggregation-prone proteins and do not influence native proteins, which are the precursors of aggregation-prone proteins. This fundamental difference in the initial rates of aggregation-prone species formation between the reaction schemes, Eqs. (5) and (25), provides another critical test to distinguish the mechanism of action of an inhibitor for the two-step model of protein aggregation. The initial rates of aggregation relative to the initial amount of native proteins are illustrated in Fig. 3.

Now that we have characterized the properties of the reversible competitive inhibition of native proteins and aggregation-prone proteins individually in the two-step model of protein aggregation, we are in the position of investigating the properties of the mixed inhibition case, where the inhibitor can act simultaneously on both the native proteins and aggregation-prone proteins. Schematically the mixed inhibition case is represented in Eq. (36). Our numerical investigations reveal that the synergistic effects of the mixed inhibition are linear, because there is both a delay in the onset of aggregation as well as decreased saturation of aggregation-prone species with increasing concentrations or strengths of the inhibitors. These properties are illustrated in Fig. 4.

5. Conditions for the validity of rapid-equilibrium approximations for the competitive inhibition reaction mechanisms

In deriving the rate equations Eqs. (22) and (34) it was assumed that the inhibitor intermediate complexes would reach a rapid-equilibrium. Under what circumstances can we use these equations? Following Hanson and Schnell [42], the derivation of the rate equations of aggregation-prone species formation under the rapid-equilibrium approximation involved two different assumptions:

Assumption I. After an initial transient, $t > t_c$, c remains approximately constant, that is, $dc/dt \approx 0$ is in the rapid equilibrium regime.

Assumption II. During the initial transient, $t < t_c$, n remains approximately constant, that is, $n \approx n_0$ before reaching the rapid equilibrium regime. This is equivalent to assuming that $a \approx 0$ during the initial transient.

The rapid-equilibrium approximation will be valid if both Assumptions I and II hold. Now let us consider these assumptions under each inhibition mechanism.

5.1. Reversible competitive inhibition of native protein

From the biophysical point of view, the Assumption I

$$\frac{dc}{dt} \approx 0 \qquad \text{for} \qquad t > t_c \tag{42}$$

can be made when the time taken for a significant change in the native protein concentration t_n (or the time taken for a significant change in the inhibitor concentration t_i) is much bigger than the time taken for a significant buildup of the intermediate complex (t_c) during the initial transient. This is equivalent to

$$\frac{t_c}{t_n} \ll 1 \qquad \text{or} \tag{43}$$

$$\frac{t_c}{t_i} \ll 1. \tag{44}$$

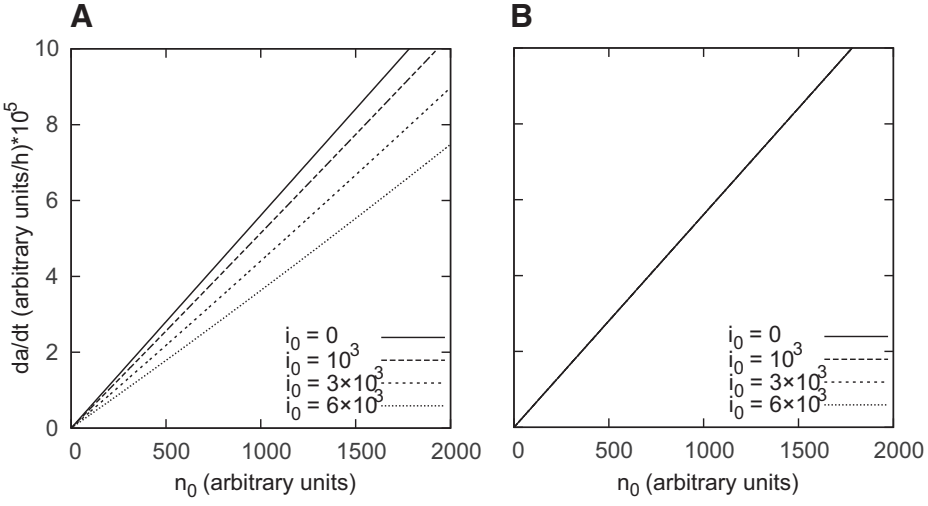

Fig. 3. Initial rate of aggregation-prone species formation v_0 for the reversible competitive inhibition of native proteins Eq. (5) [Panel A] and reversible competitive inhibition of aggregation-prone proteins Eq. (25) [Panel B]. v_0 decreases with increasing concentrations of initial inhibitor concentrations i_0 for the reversible competitive inhibition of native proteins. In contrast, v_0 is unaffected by i_0 for the reversible competitive inhibition of aggregation-prone proteins. The initial rate of these reactions is governed by Eqs. (23) and (35). The parameter values used in this figure are $k_s = 0.561 \times 10^{-7}$ and $k_i = 10^3$.

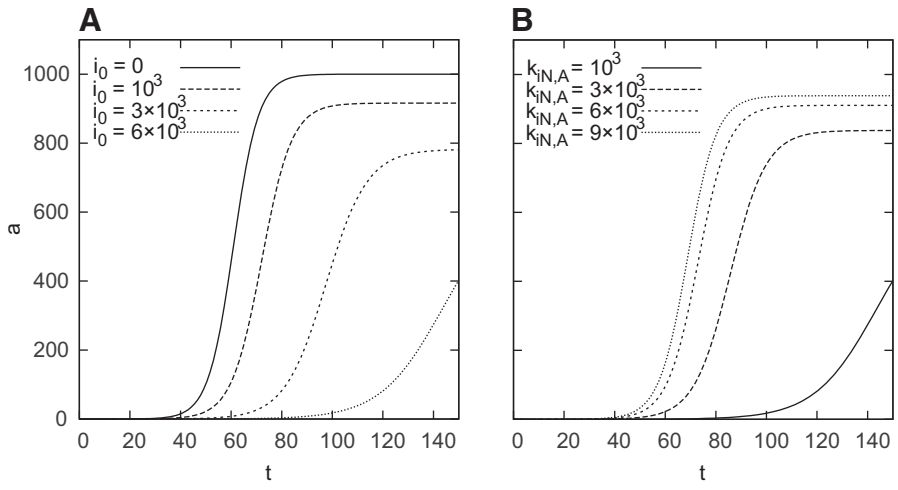

Fig. 4. Time course of the aggregation-prone species concentration a for mixed reversible competitive inhibition in the two-step model of protein aggregation Eq. (36). The inhibitor delays and decreases the formation of aggregation-prone species in the mixed inhibition [Panel A]. In [Panel B], increasing the inhibitor constants $k_{iN} = k_{dN}/k_{bN}$ and $k_{iA} = k_{dA}/k_{bA}$ also shows a reduction of the plateau and a delay in the onset of aggregation. The legend listing values of $k_{iN,A}$ indicate equal values for both k_{iN} and k_{iA}. Other parameter values used are $k_s = 1 \times 10^{-6}$, $k_f = 2 \times 10^{-4}$, $i_0 = 3000$, $a_0 = 0$, and $n_0 = 1000$. Units are arbitrary and chosen for illustrative purposes.

To calculate the initial transient timescale, t_c, we replace Eq. (13) in Eq. (9)

$$\frac{dc}{dt} = k_b n(i_0 - c) - k_d c \qquad c(0) = 0, \tag{45}$$

and solve the above differential equation by setting $n \approx n_0$. We obtain

$$c = \frac{n_0 i_0}{k_i + n_0}\left[1 - e^{-t/t_c}\right] \tag{46}$$

with

$$t_c = \frac{1}{k_d + k_b n_0}. \tag{47}$$

To calculate t_n, we adopt the timescale definition of Segel [43]:

$$t_n = \left| \frac{n_{\max} - n_{\min}}{\left.\frac{dn}{dt}\right|_{\max}} \right|. \tag{48}$$

We obtain $|dn/dt|_{\max}$ from Eq. (6) with $i = i_0 - c$, $c = (i_0\, n)/(k_i + n)$ and $n = n_0$. This value of c is obtained by applying Eq. (42) in Eq. (9). This gives $|dn/dt|_{\max} = k_s n_0$. Noting that $n_{\min} = 0$, we estimate the timescale as

$$t_n = \frac{1}{k_s}. \tag{49}$$

In a similar manner, we can calculate t_i as

$$t_i = \left| \frac{i_{\max} - i_{\min}}{\left.\frac{di}{dt}\right|_{\max}} \right|. \tag{50}$$

$|di/dt|_{\max}$ can be estimated by using Eq. (8) and assuming that $n \approx n_0$, $i \approx i_0$, and $c \approx 0$, which yields $|di/dt|_{\max} = k_b n_0 i_0$. Assuming that $i_{\min} = 0$, we obtain

$$t_i = \frac{1}{k_b n_0}. \tag{51}$$

Now replacing Eqs. (47), (49) and (51) into Eqs. (43) and (44) gives the following condition for the validity of Assumption I:

$$\frac{k_s/k_b}{k_i + n_0} \ll 1 \qquad \text{or} \tag{52}$$

$$\frac{n_0}{k_i + n_0} \ll 1. \tag{53}$$

The latter condition is always satisfied for $n_0 \ll k_i$.

Assumption II requires the native protein concentration to remain constant, that is $n \approx n_0$, during the initial transient. In mathematical terms, we define this assumption as:

$$\left|\frac{\Delta n}{n_0}\right| = \frac{t_c}{n_0}\left|\frac{dn}{dt}\right|_{t=0} \ll 1. \tag{54}$$

We already estimated t_c, so we only need to determine $|dn/dt|_{t=0}$. Applying the law of mass action and replacing $n = n_0$ to the first step ($N \to A$) of the reaction scheme Eq. (5) leads to $|dn/dt|_{t=0} = k_s n_0$. We can now expand Eq. (54) to

$$\left|\frac{\Delta n}{n_0}\right| = \frac{k_s/k_b}{k_i + n_0} \ll 1. \tag{55}$$

Note that Eq. (55) is identical to Eq. (52). In light of this, we conclude that Eq. (53) from the timescale separation assumption is, by itself, insufficient for the validity of the rapid-equilibrium approximation for the reaction scheme Eq. (5). Therefore, Eq. (52) is a stronger condition and sufficient for the validity of the rapid-equilibrium approximation.

5.2. Reversible competitive inhibition of aggregation-prone protein

For the mechanism of inhibition of aggregation-prone protein given by Eq. (25), the Assumption I, that is Eq. (42), will hold provided that

$$\frac{t_c}{t_a} \ll 1 \qquad \text{or} \tag{56}$$

$$\frac{t_c}{t_i} \ll 1. \tag{57}$$

We can estimate t_c by replacing Eq. (13) in Eq. (29)

$$\frac{dc}{dt} = k_b a(i_0 - c) - k_d c \qquad c(0) = 0, \tag{58}$$

and overestimating a at the beginning of the reaction by assuming that all n_0 has converted into a (i.e. $a \approx n_0$). Then, Eq. (58) has the same solution given by Eq. (46), which means that t_c is also given by Eq. (47).

At this point, t_a and t_i remain to be estimated to determine the conditions for Assumption I. For t_a, we again define the timescale following the approach of Segel [43]

$$t_a = \left| \frac{a_{\max} - a_{\min}}{\left.\frac{da}{dt}\right|_{\max}} \right|. \tag{59}$$

To determine $|da/dt|_{\max}$, we maximize Eq. (34) by setting $a = 0$, which yields $|da/dt|_{\max} = k_s n_0$. Noting that $a_{\min} = 0$, we estimate the timescale as

$$t_a = \frac{1}{k_s}. \tag{60}$$

In parallel to the previous analyses, it can easily be seen that, by assuming that $a \approx n_0$, $i \approx i_0$, and $c \approx 0$, t_i is identical to Eq. (51).

Replacing Eqs. (47), (51) and (60) into Eqs. (56) and (57) gives the same conditions, Eqs. (52) or (53), reported for the reversible competitive inhibition of native protein, Eq. (25).

Now we can find the condition for the validity of Assumption II. In mathematical terms, the condition is identical to Eq. (54). We already estimated t_c, so we only need to determine $|dn/dt|_{t=0}$. At the beginning of the reaction, $a = 0$. Replacing this into Eq. (26) gives $|dn/dt|_{t=0} = k_s n_0$. Upon substituting t_c and $|dn/dt|_{t=0}$ into Eq. (54), we find that the condition for the validity of Assumption II is identical to Eq. (55), which is the same condition derived for the reversible competitive inhibition of native protein.

Therefore, we conclude that Eq. (52) is sufficient for the validity of the rapid-equilibrium approximation for both the competitive inhibition of native protein and competitive inhibition of aggregation-prone protein for the two-step model of protein aggregation.

5.3. Numerical confirmation of the validity of the rapid-equilibrium approximation

We now confirm our analysis of the validity of the rapid-equilibrium approximation by comparing the approximations with the exact numerical solution to the original equations. This is illustrated in Fig. 5, where we plot the relative error introduced by the rapid equilibrium approximation in the competitive inhibition of native proteins [Eq. (22), solid line] and in the competitive inhibition of aggregation-prone proteins [Eq. (34), dashed line]. This was calculated according to the formula

$$\text{Relative Error} = \left| 1 - \frac{a_{approx}}{a_{numer}} \right| \tag{61}$$

where a_{approx} is the approximation and a_{numer} is the numerical solution. When the sufficient condition Eq. (52) for the validity of the rapid-equilibrium approximation is violated, the relative error can rise well above 0.1 (10%) for the approximation Eq. (22). In the case of Eq. (34), violation of the condition Eq. (52) resulted in a sustained relative error at approximately 0.1 (10%) as the reaction approaches equilibrium. However, the relative error is reduced (less than 0.1) when the condition Eq. (52) is valid, which occurs for a wide range of biochemically realistic rate constants. This clearly illustrates that the approximate solutions can be used to estimate kinetics parameters if our condition Eq. (52) is satisfied. We again note that condition Eq. (52) pertains to both the difference in timescales (Assumption I) and to the depletion of native protein during the initial transient (Assumption II).

6. Analysis of reversible competitive inhibition mechanisms of insulin aggregation

Now that we understand the validity of our approximations, we are in the position of using our rate equations to analyze experimental data. We focus our attention to the experimental data of insulin aggregation inhibition from Gibson and Murphy [3] and Ivanova et al. [44]. These data sets provide examples for fitting kinetic results to the F–W model with reversible competitive inhibition of native proteins Eq. (5) and reversible competitive inhibition of aggregation-prone proteins Eq. (25). Kinetic parameters were estimated using nonlinear regression algorithms implemented in Matlab R2012b (The MathWorks, Inc., Natick, MA). In our analysis, we found that the optimization

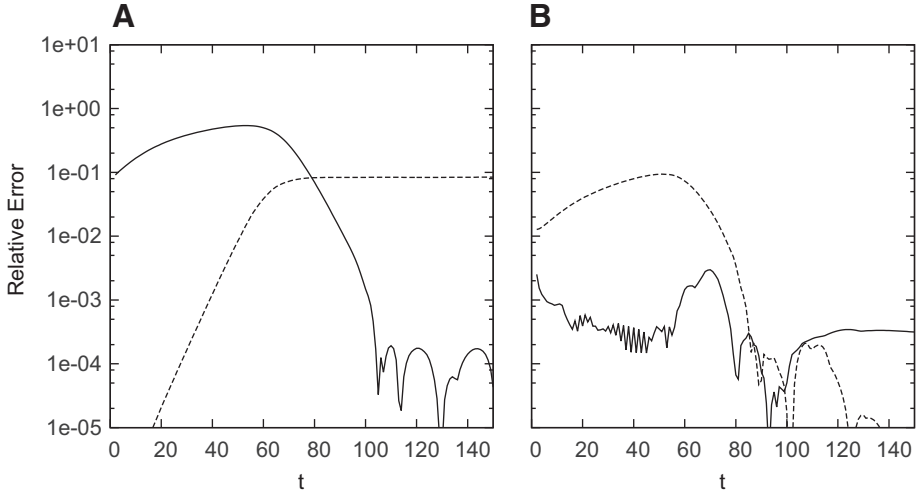

Fig. 5. Time course of the relative error, Eq. (61), between the approximations given by Eqs. (22) and (34) and the numerical solutions of Eqs. (5) and (25), which are represented as solid lines and dashed lines respectively. For both panels, we use $k_s = 1 \times 10^{-6}$, $k_f = 2 \times 10^{-4}$, $i_0 = 1000$, $a_0 = 0$, and $n_0 = 1000$. In [Panel A], $k_b = 10^{-12}$ and $k_d = 10^{-8}$, so that Eq. (52) is violated. In [Panel B], Eq. (52) is satisfied, where we use $k_b = 10^{-1}$ and $k_d = 10^{-4}$.

routine `lsqnonlin` was necessary for parameter estimations for the sparse datasets provided by Gibson and Murphy [3]. For the more plentiful data points of Ivanova et al. [44], excellent fits were obtained using the optimization routine `nlinfit`.

6.1. Reversible competitive inhibition of native insulin during insulin aggregation

In 2006, Gibson and Murphy [3] identified the short insulin fragment CGSHLVEAL which delays the aggregation of insulin. Interestingly, this fragment overlaps with an insulin domain, LVEALYLV, which has been previously proposed to be involved in insulin misfolding and aggregation [45,34]. Gibson and Murphy postulated that part or all of the B-chain segment B7–B18 of insulin, or CGSHLVEALYLV, could serve as an effective recognition or binding domain for insulin aggregation.

To investigate insulin aggregation, 0.52 mM insulin in 1 M acetic acid (pH 2.0) was incubated at 37 °C, and aliquots were taken at various time points [3]. The presence of insulin aggregation-prone species was quantified by measuring Thioflavin T (ThT) fluorescence, assuming that ThT fluorescence of insulin aggregation-prone species is proportional to the total mass of insulin aggregates in the experiment. Gibson and Murphy [3] reported a lag phase of 45–55 h, after which a rapid increase in ThT fluorescence was detected, indicating the growth of insulin aggregates.

The experimental evidence of Gibson and Murphy [3] indicates that the aggregation of insulin with and without the hybrid insulin peptides plateaus at the same value. Therefore, we use the F–W model with reversible competitive inhibition of native proteins Eq. (5) to measure the effects of hybrid peptide inhibitors in the time course of the aggregation-prone insulin formation using Gibson and Murphy's experimental data. Time course data of the aggregation-prone insulin formation is fitted to Eq. (22) in the absence of hybrid peptide inhibitors. In our analysis, we found that the Matlab optimization routine `lsqnonlin` was necessary for parameter estimations for the sparse datasets measured by Gibson and Murphy [3]. Using nonlinear regression, the k_f estimated, $k_f = (2.415 \pm 0.665) \times 10^{-4}$ (fluorescence units)$^{-1}$ (h)$^{-1}$, is excellent, but k_s shows a large deviation, $k_s = (0.561 \pm 2.597) \times 10^{-7}$ h^{-1}, which could be the result of the limited number of experimental points collected by Gibson and Murphy. With the aid of the estimated values of k_s and k_f, the inhibition constant k_i was fitted using the time course data for insulin aggregation inhibited by the hybrid peptides (see Table 1). Note that the insulin aggregation is delayed in the presence of the hybrid peptide inhibitor, but the total amount of insulin aggregates is the same obtained for the reaction in the absence of inhibitor (see Fig. 6). As shown in the Section 4, this behavior follows the distinct pattern described for the reversible competitive inhibition of native protein for the F–W model. An attempt was made to fit the data to the reaction scheme Eq. (25), which resulted in extremely poor fits (results not shown). The type of inhibition reaction is determined by the specific properties of the inhibitor molecule, and hence only reaction scheme Eq. (5) is biochemically relevant.

Table 1
The parameter values and standard errors of k_i corresponding to each inhibitory hybrid peptide. Estimates were obtained by the nonlinear fitting of Eq. (22) using the experimental data of Gibson and Murphy [3]. Insulin was dissolved at 0.52 mM in 1 M acetic acid (pH 2.0), and mixed with 2 mM hybrid peptide at 37 °C.

Hybrid peptide	k_i (fluorescence units) $\times 10^{-5}$
RRRRRR	1.844 ± 1.563
ALYLVRRRRRR	1.202 ± 0.567
GSHLVEALRRRRRR	0.175 ± 0.011
RRRRRRGSHLVEAL	0.333 ± 0.097
LVEALYLVRRRRRR	0.084 ± 0.002
RRRRRRLVEALYLV	0.050 ± 0.001

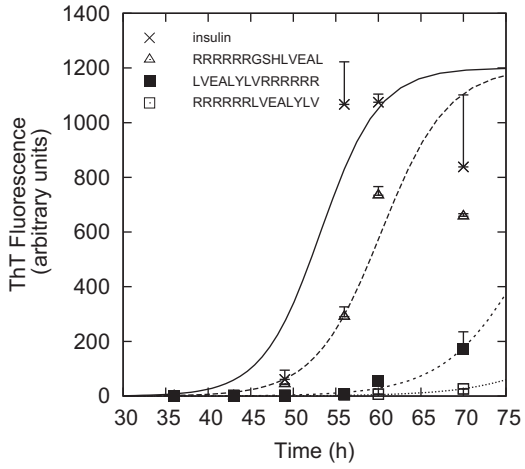

Fig. 6. Time course of insulin aggregation-prone protein formation is governed by the F–W model with reversible competitive inhibition of the insulin native protein. Using the nonlinear least squares optimization routine `lsqnonlin` from Matlab R2012b, the rate constants of the reaction Eq. (5) in the absence of inhibitor (control) were estimated as $k_s = (0.561 \pm 2.597) \times 10^{-7}$ h^{-1} and $k_f = (2.415 \pm 0.665) \times 10^{-4}$ (fluorescence units)$^{-1}$ (h)$^{-1}$. The presence of the hybrid peptide inhibitors increases the lag time of insulin aggregation-prone protein, but it does not affect the total amount of aggregation-prone insulin formed. The estimated inhibition constants are given in Table 1.

6.2. Reversible competitive inhibition of aggregation-prone insulin during insulin aggregation

In a separate study, Ivanova et al. [44] also tested the effects of short peptides (constructed from segments of insulin) on the aggregation of insulin. Non-cysteine overlapping 6-residue segments in the presence of insulin were examined to prevent any unspecific cross-linking of the interchain and intrachain disulfide bonds. Insulin and peptide were mixed in 1:1 molar ratio to a final concentration of 25 mM each in a 50 mM glycine buffer with pH 2.5. Reaction mixtures were incubated at 37 °C. The progress of the reaction was monitored by ThT fluorescence. Aliquots of the sample were removed at specified times.

The experimental time courses suggest that, although the lag times remain approximately constant, these short peptides reduce the total amount of aggregates formed. This decrease in the plateau is not due to quenching of fluorescence by the peptides, because the 8-residue peptide SLYGLENY, when co-incubated in 1:1 ratio with insulin, does

Table 2
The parameter values and standard errors of k_i corresponding to each small insulin segment. Inhibitors are listed from strongest to weakest, with GFFYTP being the most effective in reducing the total amount of aggregated species. Insulin and peptide were mixed in 1:1 molar ratio to a final concentration of 25 mM each in a 50 mM glycine buffer with pH 2.5. Reaction mixtures were incubated at 37 °C.

Small insulin segment	k_i (fluorescence units) $\times 10^{-4}$
GFFYTP	0.968 ± 0.071
HLVEAL	1.871 ± 0.127
GSHLVE	2.124 ± 0.160
EALYLV	2.149 ± 0.442
LVEALY	2.241 ± 0.180
RGFFYT	2.320 ± 0.257
FYTPKT	2.681 ± 0.408
LYQLEN	2.782 ± 0.212
VEALYL	2.806 ± 0.316
FVNQHL	3.044 ± 0.322
ERGFFY	3.077 ± 0.203
SHLVEA	3.144 ± 0.257
YQLENY	3.223 ± 0.272
FFYTPK	3.301 ± 0.386
SLYQLE	3.722 ± 0.246
GERGFF	3.931 ± 1.059

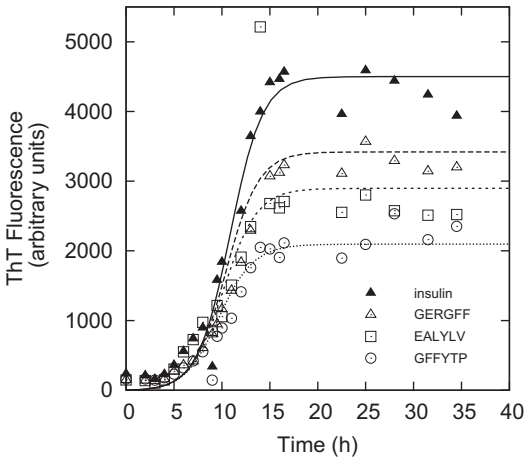

Fig. 7. Time course of insulin aggregation-prone protein formation is governed by the F–W model with reversible competitive inhibition of the aggregation-prone protein. Using nonlinear regression in Matlab R2012b, the rate constants of the reaction Eq. (25) in the absence of inhibitor (control) were estimated as $k_s = (9.636 \pm 6.185) \times 10^{-4}\ \mathrm{h}^{-1}$ and $k_f = (1.306 \pm 0.156) \times 10^{-4}\ (\text{fluorescence units})^{-1}\ (\mathrm{h})^{-1}$. The presence of the small insulin segment inhibitors decreases the total amount of aggregation-prone insulin formed, but it does not affect the lag time of insulin aggregation. The estimated inhibition constants are given in Table 2.

not have any effect on insulin aggregate formation [44]. Thus, it is reasonable to assume that the F–W model with the reversible competitive inhibition of aggregation-prone proteins is the most adequate reaction to estimate the inhibition constants of the small peptides.

Following the procedure stated in Section 6.1, we fit the experimental time course data to Eq. (34) in the absence of small insulin segments to estimate the rate constants k_s and k_f by using a nonlinear regression algorithm with the Matlab optimization routine `nlinfit`. This routine is effective for experimental data sets with a significant number of points. We estimate $k_s = (9.636 \pm 6.185) \times 10^{-4}\ (\mathrm{h})^{-1}$ and $k_f = (1.306 \pm 0.156) \times 10^{-4}\ (\text{fluorescence units})^{-1}\ (\mathrm{h})^{-1}$. Subsequently, the inhibition constant k_i was fitted using the time course data for insulin aggregation inhibited by the small insulin segments (see Table 2). Note that the aggregation is initiated at approximately the same time, but the total amount of aggregated insulin is variably reduced by the small insulin segments (see Fig. 7). The total amount of aggregated protein decreases in the presence of short peptides, which suggests that the peptides are acting on the aggregated insulin. An attempt was made to fit the data to the reaction scheme Eq. (5), which resulted in extremely poor fits (results not shown).

7. Discussion

The F–W model is widely used in the protein aggregation community. In this paper, we presented three new reversible competitive inhibition reaction mechanisms to extend the F–W model of protein aggregation Eq. (1), originally introduced by Watzky and Finke [15]. The reversible competitive inhibition mechanisms are: inhibition of native protein, inhibition of aggregation-prone protein, and inhibition of both native and aggregation-prone proteins. In these inhibition mechanisms, respectively, the inhibitor binds with high specificity to native protein, aggregation-prone protein, or both proteins. Using the rapid-equilibrium approximation, we derived simple rate equations to estimate the reaction rates and inhibition constants for the competitive inhibition of native protein and inhibition of aggregation-prone protein. In addition, we estimated the region of validity of the rapid-equilibrium approximation for the derived rate equations. This allows us to use our rate expressions to estimate the inhibition constants of time course data sets of insulin aggregation inhibition experiments of Gibson and Murphy [3] and Ivanova et al. [44].

In protein folding kinetics, the aggregation lag time is a common description of influential magnitude on protein aggregation. The F–W model Eq. (1) has been used to report lag time in aggregation experiments using estimates of the rate constant k_s. To quantify inhibitor effectiveness, researchers estimate the rate constant k_s for protein aggregation in the absence and presence of hybrid peptide inhibitors. For example, the empirical calculations by Gibson and Murphy [3] found that the hybrid insulin peptides ALYLVRRRRRR and RRRRR RGSHVEAL are comparable in their potency to delay the onset of insulin aggregation. In addition, RRRRRR and GSHVEALRRRRRR are similarly comparable in their effect on insulin aggregation. In our analysis, we were able to quantitatively characterize each inhibitor using the inhibition constant k_i. Our results suggest that longer insulin peptides are more potent in extending the lag phase, whereas shorter insulin peptides reduce the total concentration of aggregated species.

One of the core strengths of the F–W model and the F–W model with reversible competitive inhibition is their inherent simplicity. However, this minimalistic element must be considered in the context of the representative biochemical constituents and processes. The individual steps of conversion of N to A and autocatalysis of $N + A$ to $2A$ condense what could be hundreds to thousands of subsequent monomer addition events to form fibrils. In this sense, the parameters k_s and k_f are average rate constants describing this multitude of molecular events, which was also noted by Watzky and Finke [18,19,23]. Nonetheless, a more detailed model of the nucleation events would contribute to the complexity of the model, possibly preventing its analytical tractability.

Despite these limitations, we illustrate how our simplified models can be used to distinguish different mechanisms of action for protein aggregation inhibitors. We also derived initial rate expressions that can be used to estimate rate constants and inhibitor constants.

Acknowledgments

This work is supported by the University of Michigan Protein Folding Diseases Initiative and the James S. McDonnell Foundation (Grant No. 220020223) under the 21st Century Science Initiative Studying Complex Systems. MW is supported by an IRACDA Fellowship at the University of Michigan.

Appendix A. Validity of the quadratic solutions (20)–(21)

The derivation of the approximation given by Eq. (22) requires that Eq. (19) be satisfied, which we reiterate as

$$\frac{4i_0(n_0-a)}{(k_i+i_0+n_0-a)^2} \ll 1. \tag{62}$$

This expression can be written as

$$\frac{1}{i_0+n_0-a+k_i} \ll \frac{1}{2\sqrt{i_0(n_0-a)}}. \tag{63}$$

Since the denominators are both positive, we can rearrange this as

$$-\left(i_0-2\sqrt{i_0(n_0-a)}+n_0-a\right) \ll k_i \tag{64}$$

and factoring the left side then gives

$$-\left(\sqrt{i_0}-\sqrt{n_0-a}\right)^2 \ll k_i. \tag{65}$$

In these inequalities, the left side is always negative and the right side is clearly positive. As a consequence, it is appropriate to assume that condition Eq. (62) is generally valid.

References

[1] R.I. Morimoto, Proteotoxic stress and inducible chaperone networks in neurodegenerative disease and aging, Genes Dev. 22 (2008) 1427–1438.
[2] C. Hetz, L.H. Glimcher, Protein homeostasis networks in physiology and disease, Curr. Opin. Cell Biol. 23 (2011) 123.
[3] T.J. Gibson, R.M. Murphy, Inhibition of insulin fibrillogenesis with targeted peptides, Protein Sci. 15 (2006) 1133–1141.
[4] V. Sluzky, A.M. Klibanov, R. Langer, Mechanism of insulin aggregation and stabilization in agitated aqueous solutions, Biotechnol. Bioeng. 40 (1992) 895–903.
[5] V. Sluzky, J.A. Tamada, A.M. Klibanov, R. Langer, Kinetics of insulin aggregation in aqueous solutions upon agitation in the presence of hydrophobic surfaces, Proc. Natl. Acad. Sci. U. S. A. 88 (1991) 9377–9381.
[6] C. Frieden, Protein aggregation processes: in search of the mechanism, Protein Sci. 16 (2007) 2334–2344.
[7] A. Dhulesia, N. Cremades, J.R. Kumita, S.-T.D. Hsu, M.F. Mossuto, M. Dumoulin, D. Nietlispach, M. Akke, X. Salvatella, C.M. Dobson, Local cooperativity in an amyloidogenic state of human lysozyme observed at atomic resolution, J. Am. Chem. Soc. 132 (2010) 15580–15588.
[8] F. Chiti, C.M. Dobson, Amyloid formation by globular proteins under native conditions, Nat. Chem. Biol. 5 (2009) 15–22.
[9] A.R. Hurshman Babbes, E.T. Powers, J.W. Kelly, Quantification of the thermodynamically linked quaternary and tertiary structural stabilities of transthyretin and its disease-associated variants: the relationship between stability and amyloidosis, Biochemistry 47 (2008) 6969–6984.
[10] F. Oosawa, S. Asakura, Thermodynamics of the Polymerization of Protein, Academic Press, New York, NY, 1975.
[11] T.L. Hill, Y.-D. Chen, Theory of aggregation in solution. I. general equations and application to the stacking of bases, nucleosides, etc. Biopolymers 12 (1973) 1285–1312.
[12] T.L. Hill, Linear Aggregation Theory in Cell Biology, Springer-Verlag New York Inc., New York, NY, 1987.
[13] W.A. Eaton, J. Hofrichter, Hemoglobin S gelation and sickle cell disease, Blood 70 (1987) 1245–1266.
[14] P.L.S. Biagio, J. Hofrichter, A. Mozzarelli, E.R. Henry, W.A. Eaton, Current perspectives on the kinetics of hemoglobin S gelation, Ann. N. Y. Acad. Sci. 565 (1989) 53–62.
[15] M.A. Watzky, R.G. Finke, Transition metal nanocluster formation kinetic and mechanistic studies. A new mechanism when hydrogen is the reductant: slow, continuous nucleation and fast autocatalytic surface growth, J. Am. Chem. Soc. 119 (1997) 10382–10400.
[16] V.K. LaMer, R.H. Dinegar, Theory, production and mechanism of formation of monodispersed hydrosols, J. Am. Chem. Soc. 72 (1950) 4847–4854.
[17] H. Reiss, The growth of uniform colloidal dispersions, J. Chem. Phys. 19 (1951) 482.
[18] M.A. Watzky, A.M. Morris, E.D. Ross, R.G. Finke, Fitting yeast and mammalian prion aggregation kinetic data with the Finke–Watzky two-step model of nucleation and autocatalytic growth, Biochemistry 47 (2008) 10790–10800.
[19] A.M. Morris, M.A. Watzky, R.G. Finke, Protein aggregation kinetics, mechanism, and curve-fitting: a review of the literature, Biochem. Biophys. Acta Protein Proteomics 1794 (2009) 375–397.
[20] M. Kamihira, A. Naito, S. Tuzi, A.Y. Nosaka, H. Saito, Conformational transitions and fibrillation mechanism of human calcitonin as studied by high-resolution solid-state ^{13}C NMR, Protein Sci. 9 (2000) 867–877.
[21] S. Schnell, C. Mendoza, Enzyme kinetics of multiple alternative substrates, J. Math. Chem. 27 (2000) 155–170.
[22] S. Schnell, C. Mendoza, Time-dependent closed form solutions for fully competitive enzyme reactions, Bull. Math. Biol. 62 (2000) 321–336.
[23] A.M. Morris, M.A. Watzky, J.N. Agar, R.G. Finke, Fitting neurological protein aggregation kinetic data via a 2-step, minimal/Ockham's razor model: the Finke–Watzky mechanism of nucleation followed by autocatalytic surface growth, Biochemistry 47 (2008) 2413–2427.
[24] S.S.-S. Wang, Y.-T. Chen, P.-H. Chen, K.-N. Liu, A kinetic study on the aggregation behavior of β-amyloid peptides in different initial solvent environments, Biochem. Eng. J. 29 (2006) 129–138.
[25] M.-S. Lin, L.-Y. Chen, H.-T. Tsai, S.S.-S. Wang, Y. Chang, A. Higuchi, W.-Y. Chen, Investigation of the mechanism of β-amyloid fibril formation by kinetic and thermodynamic analyses, Langmuir 24 (2008) 5802–5808.
[26] R. Sabaté, M. Gallardo, J. Estelrich, An autocatalytic reaction as a model for the kinetics of the aggregation of β-amyloid, Biopolymers 71 (2003) 190–195.
[27] R. Sabaté, J. Estelrich, Stimulatory and inhibitory effects of alkyl bromide surfactants on β-amyloid fibrillogenesis, Langmuir 21 (2005) 6944–6949.
[28] R. Sabaté, U. Baxa, L. Benkemoun, N. Sánchez de Groot, B. Coulary-Salin, M.-l. Maddelein, L. Malato, S. Ventura, A.C. Steven, S.J. Saupe, Prion and non-prion amyloids of the het-s prion forming domain, J. Mol. Biol. 370 (2007) 768–783.
[29] W. Wang, Protein aggregation and its inhibition in biopharmaceutics, Int. J. Pharm. 289 (2005) 1–30.
[30] A. Knappik, A. Plückthun, Engineered turns of a recombinant antibody improve its in vivo folding, Protein Eng. 8 (1995) 81–89.
[31] R. Lundblad, R. Bradshaw, Applications of site-specific chemical modification in the manufacture of biopharmaceuticals: I. An overview, Biotechnol. Appl. Biochem. 26 (1997) 143–151.
[32] T. Arakawa, Y. Kita, J.F. Carpenter, Protein–solvent interactions in pharmaceutical formulations, Pharm. Res. 8 (1991) 285–291.
[33] S.N. Timasheff, Control of protein stability and reactions by weakly interacting cosolvents: the simplicity of the complicated, Adv. Protein Chem. 51 (1998) 355–432.
[34] J. Brange, L. Andersen, E.D. Laursen, G. Meyn, E. Rasmussen, Toward understanding insulin fibrillation, J. Pharm. Sci. 86 (1997) 517–525.
[35] M.E. Brewster, M.S. Hora, J.W. Simpkins, N. Bodor, Use of 2-hydroxypropyl-β-cyclodextrin as a solubilizing and stabilizing excipient for protein drugs, Pharm. Res. 8 (1991) 792–795.
[36] U. Grau, C.D. Saudek, Stable insulin preparation for implanted insulin pumps: laboratory and animal trials, Diabetes 36 (1987) 1453–1459.
[37] H. Thurow, K. Geisen, Stabilisation of dissolved proteins against denaturation at hydrophobic interfaces, Diabetologia 27 (1984) 212–218.
[38] P.J. Blackshear, T.D. Rohde, J.L. Palmer, B.D. Wigness, W.M. Rupp, H. Buchwald, Glycerol prevents insulin precipitation and interruption of flow in an implantable insulin infusion pump, Diabetes Care 6 (1983) 387–392.
[39] J. Brange, S. Havelund, Insulin pumps and insulin quality—requirements and problems, Acta Med. Scand. 213 (1983) 135–138.
[40] M. Katakam, A.K. Banga, Aggregation of proteins and its prevention by carbohydrate excipients: albumins and γ-globulin, J. Pharm. Pharmacol. 47 (1995) 103–107.
[41] A. Arora, C. Ha, C.B. Park, Inhibition of insulin amyloid formation by small stress molecules, FEBS Lett. 564 (2004) 121–125.
[42] S.M. Hanson, S. Schnell, Reactant stationary approximation in enzyme kinetics, J. Phys. Chem. A 112 (2008) 8654–8658.
[43] L.A. Segel, On the validity of the steady state assumption of enzyme kinetics, Bull. Math. Biol. 50 (1988) 579–593.
[44] M.I. Ivanova, S.A. Sievers, M.R. Sawaya, J.S. Wall, D. Eisenberg, Molecular basis for insulin fibril assembly, Proc. Natl. Acad. Sci. U. S. A. 106 (2009) 18990–18995.
[45] J. Brange, G. Dodson, D. Edwards, P. Holden, J. Whittingham, A model of insulin fibrils derived from the x-ray crystal structure of a monomeric insulin (despentapeptide insulin), Proteins 27 (1997) 507–516.